Dual Photocatalytic Pathways of Trichloroacetate Degradation on TiO_2: Effects of Nanosized Platinum Deposits on Kinetics and Mechanism

Soonhyun Kim and Wonyong Choi*

School of Environmental Science and Engineering, Pohang University of Science and Technology, Pohang 790-784, Korea

Received: June 3, 2002; In Final Form: August 13, 2002

The effects of nanosized platinum deposits, dioxygen, and electron donors on the kinetics and mechanism of trichloroacetate (TCA) degradation in UV-illuminated TiO_2 suspensions are described. Although platinization has been a routine method of TiO_2 modification, its effects on photocatalytic reaction mechanisms in pollutant degradation need to be fully understood. By selecting TCA as a model compound, we demonstrated that the presence of Pt deposits (typical diameters of 1−2 nm) on TiO_2 markedly changed its mechanism of photocatalytic degradation. TCA degraded photocatalytically in the presence or absence of dioxygen, which proposed that two mechanistic pathways (oxic vs anoxic) were operative. While the anoxic path was not important on bare TiO_2, it became dominant on the platinized TiO_2 surface. It is suggested that the platinum surface stabilized the reactive intermediates (e.g., dichlorocarbene) and subsequently changed the mechanistic pathway of TCA degradation. Therefore, the introduction of dioxygen in aqueous suspension enhanced the rate of TCA degradation on bare TiO_2 but inhibited it on Pt−TiO_2. The negative effect of dioxygen was much greater with platinum−rutile than platinum−anatase. The addition of excess methanol or *tert*-butyl alcohol as a hole scavenger, however, made the oxic path more favored on both bare and platinized TiO_2.

Introduction

Photocatalytic degradation reactions of an organic compound consist of a series of electron and hole transfers on illuminated TiO_2 surface, and their mechanism is very complex in general.[1] Understanding the detailed mechanistic pathways of photocatalytic reactions is critically important not only for advancing scientific knowledge about this valuable process but also for its practical application to remediation of polluted water and air. Even though the photocatalytic reaction mechanisms have been extensively studied for a variety of substrates,[1,2] the current level of understanding is still far from complete.

As an effort to increase the photonic efficiency, metalization (in particular, platinization) of TiO_2 has been a frequent topic of many photocatalytic studies on pollutant degradation.[3] However, most of the previous investigations mainly addressed the effects of Pt deposits on the photocatalytic reaction efficiency and not on the reaction mechanism. Photocatalytic reactions on platinized TiO_2 could proceed through different mechanistic pathways from those on bare TiO_2, which should be investigated in detail to get complete understanding of Pt effects.

In this study, we selected trichloroacetate (TCA) as a model compound to investigate its photocatalytic degradation kinetics and mechanism on bare and platinized TiO_2. Although there have been a few reports[4−7] on the photocatalytic degradation of TCA, detailed mechanistic investigations have not been tried. TCA represents a unique case of perchlorinated organic pollutants that have little reactivity with OH radicals.[7] Although the majority of organic pollutant degradations in the TiO_2 photocatalytic system are ascribed to the action of OH radicals,[1,2,5,8−11] the case of TCA provides a good example of how photocatalytic degradation reactions proceed without OH radicals. The photocatalytic degradation of TCA on TiO_2 could be initiated by either conduction band (CB) electron transfer (reductive path, reaction 1) or valence band (VB) hole transfer (oxidative path, reaction 2),

$$CCl_3CO_2^- + e_{cb}^- \rightarrow {}^\bullet CCl_2CO_2^- + Cl^- \quad (1)$$

$$CCl_3CO_2^- + h_{vb}^+ \rightarrow {}^\bullet CCl_3 + CO_2 \quad (2)$$

while the photo-Kolbe mechanism (reaction 2) has been previously dismissed by Choi and Hoffmann.[7] The resulting dichloroacetate radical or trichloromethyl radical rapidly reacts with dissolved O_2, leading to complete destruction with no stable intermediates produced.

$$ {}^\bullet CCl_2CO_2^- + O_2 \rightarrow {}^\bullet OOCCl_2CO_2^- \longrightarrow 2Cl^- \quad (3)$$

$$ {}^\bullet CCl_3 + O_2 \rightarrow {}^\bullet OOCCl_3 \longrightarrow 3Cl^- \quad (4)$$

On the other hand, dissolved oxygen competes with TCA for CB electrons, which in turn reduces the rate of reaction 1.

$$O_2 + e_{cb}^- \rightarrow O_2^- \quad (5)$$

Although dissolved oxygen seems to be essentially required for the photocatalytic degradation of TCA according to the above reactions, its degradation in the absence of O_2 was known from the previous studies.[4,7] The anoxic mechanism needs to be elucidated.

This study aims to find out what the anoxic mechanism is, how the presence of Pt deposits on TiO_2 affects the mechanism, and what experimental parameters change the mechanism of TCA degradation. The photocatalytic degradation of TCA was demonstrated both in the presence and in the absence of

* To whom correspondence should be addressed. E-mail: wchoi@postech.ac.kr.

10.1021/jp0262261 CCC: $22.00 © 2002 American Chemical Society
Published on Web 12/04/2002

dioxygen. The dual pathways of TCA degradation were proposed in this study. By comparing the kinetics and product distributions of TCA photodegradation on anatase, rutile, and its platinized counterparts under different experimental conditions, we were able to deduce the mechanistic pathways and understand the deciding parameters.

Experimental Section

Materials and Chemicals. $CHCl_2CO_2Na$ (Aldrich), CCl_3CO_2Na (Aldrich), methanol (Aldrich), and *tert*-butyl alcohol (Shinyo) were used as received. The water used was ultrapure (18 MΩ cm) and prepared by a Barnstead purification system. Titanium dioxide (Degussa P25) of mostly anatase (80% anatase and 20% rutile) with an average surface area of 50 ± 15 m^2/g was used as photocatalyst. Other chemicals used were of the highest purity available.

Rutile TiO_2 powder was prepared from selectively etching out the anatase portion of P25 TiO_2 by HF solution (10 wt %).[12] The fluoride contaminants adsorbed on the rutile surface were removed by washing with alkaline (1 N NaOH) solution. By this method, rutile powder with comparable particle size to P25 could be obtained. X-ray powder diffraction analysis (Rigaku model D/Max III) with Cu $K\alpha_1$ radiation was performed to measure the phase content and the particle size of TiO_2 samples. The (101) peak of anatase and the (110) peak of rutile were used for analysis. The rutile content before and after HF treatment, which was calculated from the ratio of peak heights,[13] was 17% and 82%, respectively. The particle sizes that were estimated from X-ray peak width (using Scherrer equation) were 26 nm for P25 (mostly anatase) and 30 nm for the HF-etched P25 (mostly rutile). The Brunauer−Emmett−Teller (BET) surface area measurements of powder samples were carried out by using N_2 as an adsorptive gas. The measured values were 52 and 40 m^2/g for P25 and HF-etched P25, respectively. Platinized TiO_2 was obtained using a photodeposition method.[14−16] Titanium dioxide (0.5 g/L) suspension with 1 M methanol (electron donor) and 0.1 mM chloroplatinic acid (H_2PtCl_6) was irradiated with a 200-W medium-pressure mercury lamp for 30 min. After irradiation, Pt-deposited TiO_2 powder was filtered, washed with distilled water, and dried under air. A typical Pt loading on TiO_2 was estimated to be ca. 0.2 wt %. Transmission electron microscopic (TEM) images of Pt−TiO_2 sample showed that Pt particles with a size range of 1−2 nm were well dispersed on TiO_2 particles (20−30 nm diameter). Throughout this paper, P25 TiO_2 will be referred to as anatase (A), HF-etched P25 as rutile (R), and their platinized counterparts as Pt−A and Pt−R, respectively.

Photolyses and Analyses. All TiO_2 suspensions were prepared at a concentration of 0.5 g/L and were dispersed by simultaneous sonication and shaking for 30 s in an ultrasonic cleaning bath. An aliquot of TCA stock solution (10 mM) was subsequently added to the suspension to give a desired concentration (1 mM), and then the pH of the suspension was adjusted with HNO_3 or NaOH standard solution. For experiments in the absence of dissolved O_2, the reactor was continuously purged with nitrogen gas before and during the photolysis. Photoirradiation employed a 1000-W Xe arc lamp (Oriel) as a light source. Light passed through a 10-cm IR water filter and a UV cutoff filter ($\lambda > 300$ nm), and then the filtered light was focused onto a 30-mL Pyrex reactor with a quartz window. The reactor was filled with minimized headspace, sealed with a rubber septum, and stirred magnetically. Sample aliquots were withdrawn by a 1-mL syringe and filtered through a 0.45-μm PTFE filter (Millipore). A set of duplicate or triplicate experiments was carried out for each photolysis.

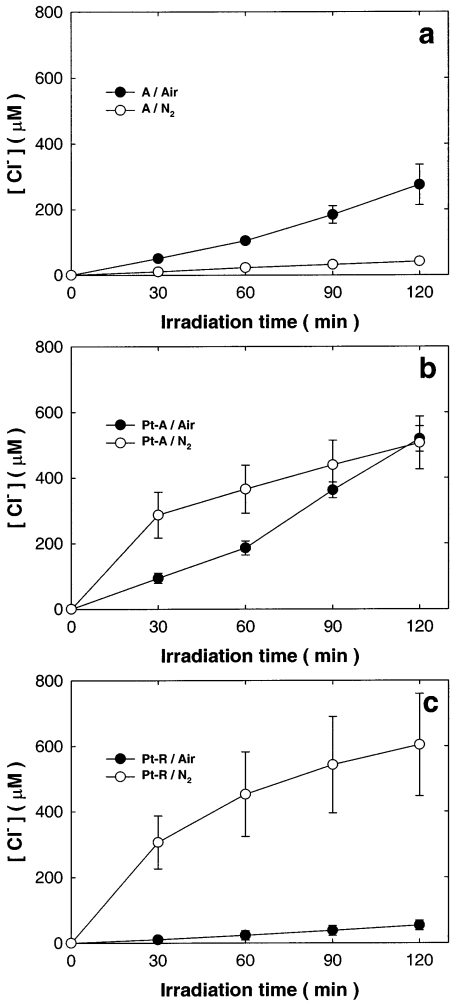

Figure 1. Time-dependent chloride production profiles from the photocatalytic degradation of 1 mM TCA with different photocatalysts under air- or nitrogen-saturated suspensions at pH 3: (a) anatase; (b) Pt−A; (c) Pt−R.

Identification and quantification of ionic intermediates and products were performed using an ion chromatograph (IC, Dionex DX-120) that was equipped with a Dionex IonPac AS 14 (4 mm × 250 mm) for anion analysis and a conductivity detector. The eluent solution was 3.5 mM Na_2CO_3/1 mM $NaHCO_3$.

Results and Discussion

Effects of Platinum Deposits and Dioxygen. Figure 1 shows the time-dependent chloride production from the photocatalytic degradation of TCA in the presence or absence of dioxygen with different TiO_2 photocatalysts at pH 3. Each photocatalyst exhibited a quite different reactivity dependent on dioxygen. The presence of O_2 had a strong positive effect on the anatase (A) activity, a moderately negative effect on the Pt−A activity, and a strong negative effect on the Pt−R activity. Initial chloride production rate decreased in the order of Pt−$R/N_2 \approx$ Pt−A/N_2 > Pt−A/air > A/air > Pt−R/air ≈ A/N_2. Table 1 summarizes the results of photocatalytic degradation of TCA with four different TiO_2 photocatalysts (A, R, Pt−A, Pt−R) under four different experimental conditions (pH 3/air, pH 3/N_2, pH 10/air, pH 10/N_2). Photoreactivities were compared between pH 3 and 10, at which the surface charge of TiO_2 particles was positive and negative, respectively. Rutile (R) data is missing in this table because it did not show any measurable reactivity

TABLE 1: Products and Intermediates Formation (μM) from the Photocatalytic Degradation of TCA (1 mM) with Different TiO_2 Photocatalysts and Experimental Conditions

		air					N_2				
photocatalyst	time (min)	TCA	DCA[a]	Cl^-	r[b]	total Cl (%)	TCA	DCA[a]	Cl^-	r[b]	total Cl (%)
					pH 3						
anatase	0	958	0	0		100	953	0	0		100
	30	947	0	56	0	101	949	9	9	1.00	101
	60	925	0	101	0	100	959	22	22	1.00	103
	90	906	0	165	0	100	945	32	32	1.00	103
	120	898	0	231	0	102	944	43	43	1.00	104
Pt−A	0	1043	0	0		100	1030	0	0		100
	30	1010	0	94	0	100	879	70	287	0.24	99
	60	975	0	186	0	99	848	78	365	0.21	99
	90	939	0	362	0	102	832	82	439	0.19	100
	120	880	0	519	0	101	824	81	506	0.16	102
Pt−R	0	1033	0	0		100	984	0	0		100
	30	1023	2	10	0.20	99	875	98	306	0.32	106
	60	1010	3	23	0.13	99	755	140	453	0.31	102
	90	1001	3	38	0.08	98	702	152	543	0.28	100
	120	994	2	54	0.04	98	686	183	604	0.30	103
					pH 10						
anatase	0	984	0	0		100	895	0	0		100
	30	954	1	15	0.07	98	912	9	9	1.00	103
	60	975	2	14	0.14	100	899	18	22	0.82	103
	90	945	1	14	0.07	97	885	34	32	1.06	103
	120	948	4	15	0.27	97	889	41	43	0.95	104
Pt−A	0	1033	0	0		100	1047	0	0		100
	30	1020	0	22	0	99	995	16	138	0.12	100
	60	1012	0	27	0	99	978	18	187	0.10	101
	90	1021	0	31	0	100	970	19	218	0.09	101
	120	1015	0	37	0	99	950	24	250	0.10	100
Pt−R	0	978	0	0		100	970	0	0		100
	30	961	0	0	0	98	961	0	126	0	103
	60	976	0	1	0	100	952	0	157	0	104
	90	972	0	5	0	100	951	0	186	0	104
	120						945	0	214	0	105

[a] Dichloroacetate. [b] $r = [DCA]/[Cl^-]$.

with TCA under both air- and N_2-saturated conditions. Dichloroacetate (DCA) was formed as an intermediate, which should result from net two-electron transfers to TCA (reaction 1 + reaction 6).

$$^{\bullet}CCl_2CO_2^- + e_{cb}^- + H^+ \rightarrow CHCl_2CO_2^- \qquad (6)$$

The two-electron-transfer process (i.e., DCA formation) was favored with Pt−TiO_2 and almost completely hindered in the presence of O_2. Therefore, DCA formation was significant only in the N_2-saturated suspension, in which the chloride production rate gradually decelerated with the accumulation of DCA. This indicates that reaction 6 was not fast enough to compete with the addition of O_2 (reaction 3). Bahnemann et al.[16] also observed that the net two-electron transfer to halothane was highly favored on photoplatinized TiO_2 and decreased with increasing dioxygen concentration. Because the total chlorine balance was satisfactorily met for all cases, there should be no other chlorine-containing intermediates in TCA degradation.

The general features shown in Table 1 can be described as follows. First, TCA degradation was sensitively influenced by the bulk and surface structure of TiO_2. TCA degraded on anatase but not on rutile at all. Platinization of both anatase and rutile significantly enhanced their reactivity. Different photoreactivities should be understood in terms of the efficiency of the initial electron transfer to TCA (reaction 1). Rutile has a slightly less negative CB edge potential than anatase (-0.3 vs -0.5 V_{NHE})[17] and thus is less likely to transfer CB electrons to TCA of which the half-wave reduction potential is -0.49 V (vs NHE).[18] Platinization that reduces the electron−hole pair recombination rate through Schottky-barrier CB electron trapping is expected to increase the rate of electron transfer (reaction 1). Although rutile was not able to dechlorinate TCA at all, the reactivity of Pt−R was comparable to or even higher than Pt−A under N_2 saturation. Second, TCA degradation rate at pH 10 was significantly reduced from the rate at pH 3 or almost completely inhibited. This was previously explained in terms of the electrostatic surface charge model:[6] the negative surface charge on TiO_2 at pH 10 ($pH_{zpc} \approx 6.4$)[19] repels TCA anions. Third, the effect of dioxygen on the degradation rate was positive only with the anatase at pH 3 but negative with the other cases. Because the dioxygen serves as both a reactant (reactions 3 and 4) and a competing electron acceptor (reaction 5), the effect of O_2 should be explained in terms of its dual roles.[20] Finally, it should be noted that the anoxic degradation of TCA was drastically enhanced with platinized TiO_2. The reaction of DCA radical with VB holes (reaction 7) could be responsible for this anoxic pathway.[7]

$$^{\bullet}CCl_2CO_2^- + h_{vb}^+ \rightarrow CCl_2 + CO_2 \qquad (7)$$

The resulting dichlorocarbene (CCl_2) could be hydrolyzed to yield chloride ions in an anoxic solution.[20,21] Dichlorocarbene as a transient intermediate was previously shown to exist during the photocatalytic degradation of CCl_4 on TiO_2.[20] When the anoxic path (reaction 1 + reaction 7) is dominant, the presence of O_2 reduces the reactivity by scavenging CB electrons (reaction 5) as in the case of Pt−A and Pt−R (Figure 1 and Table 1). However, this anoxic mechanism seems to be effective only in the presence of Pt deposits.

SCHEME 1: Two Proposed Mechanistic Paths of Photocatalytic Degradation of TCA on TiO_2 with or without Dioxygen[a]

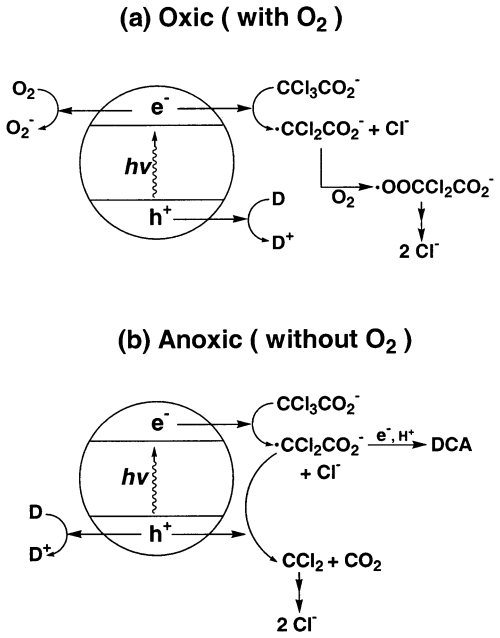

[a] D stands for electron donors (hole-scavengers), which could be water molecules, surface hydroxyl groups, or added alcohols (MeOH, *t*-BuOH).

On the basis of the above argument, we propose that two paths (oxic vs anoxic) are competing for TCA degradation on illuminated TiO_2. They are pictorially compared in Scheme 1. The effects of various parameters (e.g., platinization, crystalline phase, electron donor, dioxygen) on TCA degradation rate should be understood in terms of which path a specific condition favors. The effects of O_2 were positive or negative depending on the kind of photocatalyst. Dioxygen is essential for the oxic path as a reagent, whereas it competes for CB electrons with TCA to reduce the reactivity in the anoxic path. Therefore, dioxygen would enhance the reactivity when the oxic mechanism is dominant, while the opposite effect should be observed with the anoxic mechanism in action. The reactivity of anatase was much enhanced with dioxygen, which indicated that the oxic path predominated on anatase. The anoxic mechanism should be favored with platinized TiO_2 because its reactivity was reduced in the presence of dioxygen. This implies that the kinetics of electron transfers to O_2 and TCA on bare TiO_2 surface is quite different from those on Pt−TiO_2 (reactions 8−11).

$$TiO_2\,(e_{cb}^-) + O_2 \rightarrow O_2^- \quad (8)$$

$$TiO_2\,(e_{cb}^-) + TCA \rightarrow {}^\bullet CCl_2CO_2^- + Cl^- \quad (9)$$

$$Pt\,(e_{cb}^-) + O_2 \rightarrow O_2^- \quad (10)$$

$$Pt\,(e_{cb}^-) + TCA \rightarrow {}^\bullet CCl_2CO_2^- + Cl^- \quad (11)$$

The fact that the electron-transfer rate to O_2 was much faster on platinized TiO_2 than on bare TiO_2 is known.[3a−c,22] The rate of electron transfer to TCA is also expected to increase on Pt−TiO_2 in a similar way. Therefore, the effect of O_2 on the TCA degradation rate should depend on the rate ratio of electron transfers to O_2 and TCA. Judging from the kinetic results, reaction 10 should be faster than reaction 11 on Pt−TiO_2, whereas reaction 8 is not fast enough to compete with reaction 9 on bare TiO_2. The competing electron transfers on Pt−TiO_2 surface are compared in Scheme 2. The interfacial electron transfers can take place on two different sites: naked TiO_2 vs Pt surface. In the absence of O_2, most electrons transfer to TCA on Pt sites and not on naked TiO_2 surface ($r_{Pt-TCA} \gg r_{A-TCA} > r_{R-TCA} \approx 0$) because the anoxic TCA degradation rates were greatly enhanced with platinization. When O_2 was present, on the other hand, electrons on Pt should transfer to both O_2 and TCA because dioxygen was detrimental to the activity of Pt−TiO_2. It should be also noted that the effects of platinization were markedly different between the anatase and the rutile. The negative effect of dioxygen was more prominent with Pt−R than Pt−A (Figure 1b,c), which implied that the ratio, r_{Pt-O_2}/r_{Pt-TCA}, was much higher with Pt−R than Pt−A. The different effects of platinization between the anatase and the rutile were also observed in a study of photocatalytic oxidation of 2-propanol to acetone, where the Pt deposits had a beneficial effect for rutile and a detrimental effect for anatase.[15b]

Effects of Organic Electron Donors. According to Scheme 1, electron donors (or hole scavengers) should enhance the oxic path and suppress the anoxic path. The results of photocatalytic degradation of TCA in the presence of organic electron donors [methanol (MeOH) and *tert*-butyl alcohol (*t*-BuOH)] are summarized in Table 2, which is directly comparable with Table 1 for each photocatalyst. It is noteworthy that Pt−A was particularly effective in degrading TCA in the presence of electron donors. Unlike the case of Table 1, the introduction of dioxygen with electron donors increased the degradation rate for all photocatalysts tested. This implied that the oxic path was more important than the anoxic path in the presence of excess electron donors. This might be because electron donors scavenge VB holes and reduce the rate of reaction 7. DCA formation was also highly enhanced in the presence of electron donors (compare Tables 1 and 2). Electron donors scavenge VB holes, which in turn enhance the two-electron transfer to TCA to produce DCA. They also serve as a H-atom donor to the DCA radical to generate DCA.

$$CH_3OH + {}^\bullet CCl_2CO_2^- \rightarrow {}^\bullet CH_2OH + CHCl_2CO_2^- \quad (12)$$

Because the resulting hydroxymethyl radical ($^\bullet CH_2OH$) is a strong reductant ($E_{1/2} = -0.97$ V vs NHE),[23] it could affect the reduction process of TCA by initiating a series of chain reactions.

$$ {}^\bullet CH_2OH + TiO_2 \rightarrow HCHO + H^+ + TiO_2\,(e_{cb}^-) \quad (13)$$

$$ {}^\bullet CH_2OH + CCl_3CO_2^- \rightarrow HCHO + H^+ + Cl^- + {}^\bullet CCl_2CO_2^- \quad (14)$$

$$ {}^\bullet CH_2OH + {}^\bullet CCl_2CO_2^- \rightarrow HCHO + CHCl_2CO_2^- \quad (15)$$

Therefore, the interpretation of the reactivity data in the presence of MeOH (Table 2) should be complicated.

In Table 2, *t*-BuOH, which does not have such secondary effects, is also compared with MeOH. Following a H-atom abstraction, *t*-BuOH transforms into a dimerized product, 2,5-dimethylhexane-2,5-diol under N_2 saturation.[24] Figure 2a shows the effect of *t*-BuOH concentration on the photocatalytic TCA dechlorination at pH 3. The presence of *t*-BuOH should enhance the oxic path because it scavenges VB holes (Scheme 1a) as is the case for Pt−A/air. As for the anoxic path (Scheme 1b), the

SCHEME 2: Competing CB Electron Transfers to TCA and O_2 on Pt−TiO_2[a]

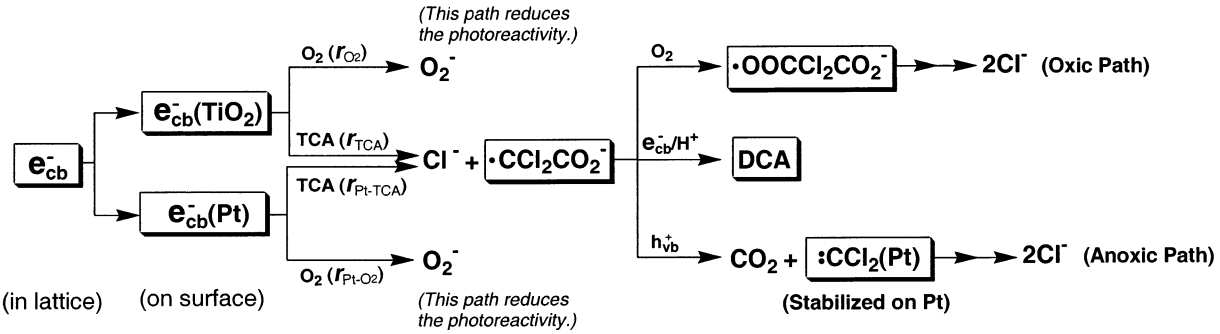

[a] The electrons generated in the bulk lattice diffuse onto the two different surface sites (naked TiO_2 vs Pt) where subsequent electron transfers to TCA or O_2 take place. The CB electron transfer to O_2 reduces the photocatalytic degradation of TCA.

TABLE 2: Products and Intermediates Formation (μM) from the Photocatalytic Degradation of TCA (1 mM) in the Presence of Electron Donors, MeOH or *t*-BuOH[a]

		air					N_2				
photocatalyst	time (min)	TCA	DCA	Cl^-	*r*	total Cl (%)	TCA	DCA	Cl^-	*r*	total Cl (%)
					MeOH (10 mM)						
A	0	1087	0	0		100	944	0	0		100
	30	1065	0	88	0.00	101	945	1	4	0.25	100
	60	1030	9	188	0.05	101	942	4	9	0.44	100
	90	1006	19	306	0.06	103	940	10	18	0.56	101
	120	945	26	468	0.06	103	933	15	30	0.50	101
R	0	1094	0	0		100	1113	0	0		100
	30	1092	5	19	0.26	101	1093	1	1	1.00	98
	60	1072	12	70	0.17	101	1087	4	4	1.00	98
	90	1036	19	122	0.16	100	1066	10	12	0.83	97
	120	1043	23	164	0.14	102	1058	23	28	0.82	97
Pt−A	0	1012	0	0		100	1042	0	0		100
	30	705	231	646	0.36	106	872	127	315	0.40	102
	60	400	502	984	0.51	105	692	255	664	0.38	104
	90	139	693	1475	0.47	108	524	404	1011	0.40	109
	120	20	733	1791	0.41	109	380	534	1330	0.40	113
Pt−R	0	986	0	0		100	1006	0	0		100
	30	848	68	385	0.18	104	936	45	84	0.54	99
	60	675	136	629	0.22	99	921	65	126	0.52	100
	90	569	169	952	0.18	101	897	85	172	0.49	100
	120	482	173	1236	0.14	102	877	116	229	0.51	102
					t-BuOH (10 mM)						
A	0	983	0	0		100	960	0	0		100
	30	963	4	41	0.10	100					
	60	934	10	123	0.08	100	927	24	28	0.86	99
	90	906	15	201	0.07	100	907	32	45	0.71	98
	120	877	23	299	0.08	101	902	28	61	0.46	98
Pt−A	0	1007	0	0		100	1042	0	0		100
	10	944	7	172	0.04	100	891	83	208	0.40	97
	20	730	86	804	0.11	105	825	133	294	0.45	97
	30	553	121	975	0.12	95	790	159	345	0.46	97
	60	364	105	1605	0.07	96	734	193	459	0.42	97
	90	312	37	1857	0.02	95	702	200	529	0.38	97
	120	295	20	2042	0.01	98	684	215	592	0.36	98
Pt−R	0						980	0	0		100
	30						831	125	257	0.49	102
	60						747	165	372	0.44	100
	90						718	218	436	0.50	103
	120						673	258	485	0.53	103

[a] Other experimental conditions were the same as those of Table 1. The pH of the suspensions was 3.

effect of *t*-BuOH on the reactivity should be positive when reaction 1 is enhanced by VB hole scavenging or negative when reaction 7 is blocked by excess hole scavengers. The fact that *t*-BuOH had little effect on the dechlorination rate up to [*t*-BuOH] = 10^{-2} M under N_2 saturation implied that the two effects were counterbalanced. However, with [*t*-BuOH] > 10^{-2} M the positive effect dominated. The decrease of chloride production at excessive [*t*-BuOH] should be ascribed to the competition for the surface sites between TCA and *t*-BuOH.[25] Figure 2b shows the ratio of r = [DCA]/[Cl^-] as a function of [*t*-BuOH]. The ratio, *r*, should be taken as an indicator of the degree of TCA mineralization. At $r = 0$, TCA is completely mineralized, whereas it is quantitatively converted into DCA at $r = 1$. With increasing [*t*-BuOH], *r* gradually increased with

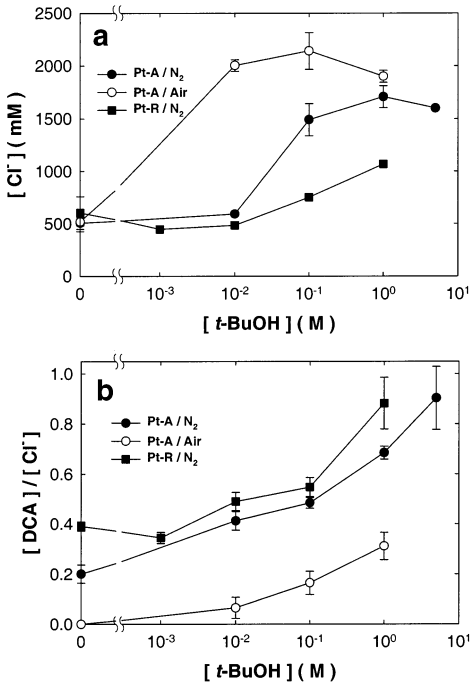

Figure 2. Effect of *t*-BuOH on the photocatalytic degradation of TCA (1 mM) with Pt−A and Pt−R at pH 3: (a) chloride production after 2-hr illumination as a function of [*t*-BuOH]; (b) the ratio of [DCA] to [Cl^-] as a function of [*t*-BuOH].

TABLE 3: Qualitative Comparison of the TCA Degradation Rates (with Respect to a Reference Condition) among Different Reaction Conditions[a]

A. Relative Reactivity under Four Different Conditions for Each Photocatalyst

	A	Pt−A	R	Pt−R
N_2	Ref	Ref	Ref	Ref
O_2	++	−	O	− −
N_2 + MeOH	O	++	+	−
O_2 + MeOH	++	++	+	++
N_2 + *t*-BuOH	+	+	O	O
O_2 + *t*-BuOH	++	++	O	

B. Relative Reactivity among Four Different Photocatalysts for a Given Condition

	A	Pt−A	R	Pt−R
N_2	Ref	++	−	++
O_2	Ref	+	− −	−
N_2 + MeOH	Ref	++	O	+
O_2 + MeOH	Ref	++	−	++
N_2 + *t*-BuOH	Ref	++	−	++
O_2 + *t*-BuOH	Ref	++	−	

[a] Ref = reference condition or photocatalyst; O = little change of the degradation rate with respect to Ref; + = increase; ++ = significant increase; − = decrease; − − = significant decrease.

less mineralization. The degree of TCA mineralization was obviously higher (with lower *r* values) in the presence of dioxygen.

Because the photocatalytic reactivities (TCA degradation) shown in Tables 1 and 2 vary in a complex way with different photocatalysts and conditions, the results are simplified and compared qualitatively in Table 3. Table 3, section A, compares the degradation rates under different conditions for each photocatalyst with respect to a reference condition (N_2 saturation) and Table 3, section B, compares the reactivity of different photocatalysts at a given condition with respect to a reference photocatalyst (anatase). The qualitative effect of a specific parameter could be understood on the basis of the proposed mechanism. For example, the effect of methanol (hole scavenger) was positive or negative depending on the kind of photocatalysts. According to Scheme 1, the presence of methanol boosts the oxic path by scavenging VB holes, and thus the methanol effects are all positive when the oxic path prevails in the presence of oxygen (Table 3A). On the other hand, methanol in the absence of oxygen could make the anoxic path unfavored when reaction 7 is blocked with excess hole scavengers (the case of Pt−R) or could enhance the anoxic path when the enhancing effect of electron transfer to TCA through reactions 1 and 14 is more important (the case of Pt−A and R). As for the relative reactivities among different photocatalysts, Pt−R was a better photocatalyst than the anatase (A) for all reaction conditions except the case of air-saturated suspension (see the O_2 row in Table 3, section B). On Pt−R, the rate of CB electron transfer to O_2 must be much faster than that to TCA.

The Fate of DCA Radicals on Bare and Platinized TiO_2. Because the initial step of TCA degradation produces the DCA radical (reaction 1), the fate of DCA radicals on TiO_2 is critical in determining the overall mechanistic pathway. Once the DCA radical is generated, it can have three branching pathways as shown in Scheme 2: (1) reaction with CB electrons to produce DCA (reaction 6); (2) reaction with VB holes (reaction 7); (3) reaction with O_2 (reaction 3). Therefore, the actual pathway should depend on the relative rates of the elementary reactions. The rate ratios, as mentioned in the previous section, should also depend on the kind of TiO_2 surface: bare and platinized. As shown in Table 1, DCA radicals did not react with holes (reaction 7) at all on bare TiO_2 surface, which stoichiometrically converted only to DCA (reaction 6) under the anoxic condition ($r = 1.0$). However, the path (reaction 7) opened on Pt−TiO_2 surface. With both Pt−A and Pt−R, the *r* values (0.2−0.3) in the anoxic condition were significantly lower than 1.0, which implied that most DCA radicals were mineralized through reaction 7. Therefore, it is concluded that reaction 7 is highly favored over reaction 6 on Pt−TiO_2, whereas it (reaction 7) is absent on bare TiO_2. The presence of Pt deposits on TiO_2 not only accelerates the rate of CB electron transfer (reaction 1) but also changes the mechanistic pathway by stabilizing reactive intermediates. The fact that DCA radicals were preferentially mineralized on Pt−TiO_2 rather than converted to DCA implied that dichlorocarbenes (produced from reaction 7) should be highly stabilized on the Pt surface. This should explain why the anoxic degradation of TCA was effective only with Pt−TiO_2.

To verify the anoxic pathway of DCA radicals on Pt−TiO_2, photocatalytic degradation reaction of DCA was investigated by comparing its reactivity under oxic and anoxic conditions. The reaction of DCA with OH radicals (reaction 16) provides an alternative pathway to DCA radicals.

$$CHCl_2CO_2^- + {}^\bullet OH \rightarrow {}^\bullet CCl_2CO_2^- + H_2O \qquad (16)$$

Once the DCA radical is produced through this path, both oxic and anoxic paths of Scheme 1 could follow as in the case of TCA degradation. As shown in Figure 3a, the photocatalytic degradation of DCA in the presence of dioxygen was achieved with a complete mineralization (reaction 17)[26] on both bare and platinized TiO_2.

$$CHCl_2CO_2^- + O_2 \rightarrow 2CO_2 + H^+ + 2Cl^- \qquad (17)$$

The degradation rate was much faster on Pt−TiO_2. Because DCA does not react directly with CB electrons, the Pt-enhanced

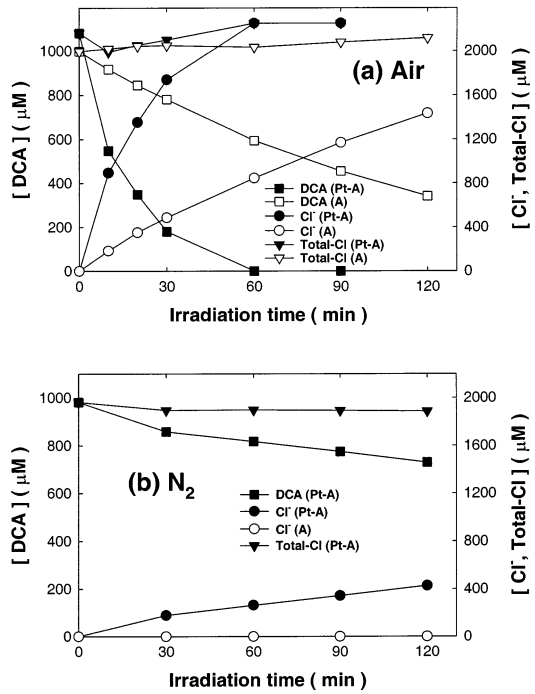

Figure 3. Photocatalytic degradation of DCA and the chloride production on the anatase (A) and Pt−A at pH 3 under (a) air-saturated and (b) N_2-saturated suspension.

effect should be ascribed either to the reduced electron−hole pair recombination with increasing the rate of reaction 16 or to the stabilization of DCA radicals on the Pt surface. On the other hand, the anoxic photodegradation of DCA on the anatase (Figure 3b) was not observed at all, unlike the case of TCA, because the CB acceptors (e.g., TCA, O_2) were absent. However, the anoxic degradation of DCA on Pt−A did proceed with a reduced rate (Figure 3b) because protons could be an alternative CB electron acceptor on the Pt surface (reaction 18).[27,28]

$$H^+ + Pt\,(e_{cb}^-) \rightarrow {}^1/_2H_2 \qquad (18)$$

As a result, DCA radicals could be degraded through reaction 7 in the absence of dioxygen. It is verified, therefore, that DCA radicals generated from a different source can also follow an anoxic path through reacting with VB holes on Pt−TiO_2.

Conclusions

In this study, we demonstrated that the platinization of TiO_2 significantly changed the mechanistic pathways of TCA degradation. While the anoxic degradation path was minor on bare TiO_2, it became dominant on platinized TiO_2 surface. As a result, the presence of dioxygen enhanced the TCA degradation on bare TiO_2 but inhibited it on platinized TiO_2. On the other hand, the addition of excess organic electron donors made the oxic path favored on both bare and platinized TiO_2 by scavenging VB holes. This study presents a unique example that a recalcitrant organic pollutant could be successfully degraded in an anoxic environment using platinized TiO_2 photocatalyst. Although the platinization of TiO_2 has been a common modification method for enhancing its photocatalytic activity, the mechanistic aspects of Pt modification should be properly addressed and understood for its application to environmental remediation.

Acknowledgment. We appreciate the financial supports from Ministry of Education through the Brain Korea 21 project and KOSEF through the Center for Integrated Molecular Systems.

References and Notes

(1) Hoffmann, M. R.; Martin, S. T.; Choi, W.; Bahnemann, D. W. *Chem. Rev.* **1995**, *95*, 69.
(2) (a) Choi, W.; Hong S. J.; Chang, Y.-S.; Cho, Y. *Environ. Sci. Technol.* **2000**, *34*, 4810. (b) Choi, W.; Ko, J. Y.; Park, H.; Chung, J. S. *Appl. Catal. B* **2001**, *31*, 209. (c) Cho, S.; Choi, W. *J. Photochem. Photobiol., A* **2001**, *143*, 221. (d) Kim, S.; Choi, W. *Environ. Sci. Technol.* **2002**, *36*, 2019. (e) Cho, Y.; Choi, W. *J. Photochem. Photobiol. A*, **2002**, *148*, 129. (f) Lee, H.; Choi, W. *Environ. Sci. Technol.* **2002**, *36*, 3872.
(3) (a) Izumi, I.; Dunn, W. W.; Wilbourn, K. O.; Fan, F. R.; Bard, A. J. *J. Phys. Chem.* **1980**, *84*, 3207. (b) Gerischer, H.; Heller, A. *J. Phys. Chem.* **1991**, *95*, 5261. (c) Wang, C.-M.; Heller, A.; Gerischer, H. *J. Am. Chem. Soc.* **1992**, *114*, 5230. (d) Driessen, M. D.; Grassian, V. H. *J. Phys. Chem. B* **1998**, *102*, 1418. (e) Einaga, H.; Futamura, S.; Ibusuki, T. *Environ. Sci. Technol.* **2001**, *35*, 1880. (f) Subramanian, V.; Wolf, E.; Kamat, P. V. *J. Phys. Chem. B* **2001**, *105*, 11439.
(4) Chemseddine, A.; Boehm, H. P. *J. Mol. Catal.* **1990**, *60*, 295.
(5) Mao, Y.; Schöneich, C.; Asmus, K.-D. *J. Phys. Chem.* **1991**, *95*, 10080.
(6) Kormann, C.; Bahnemann, D. W.; Hoffmann, M. R. *Environ. Sci. Technol.* **1991**, *25*, 494.
(7) Choi, W.; Hoffmann, M. R. *Environ. Sci. Technol.* **1997**, *31*, 89.
(8) Truchi, C. S.; Ollis, D. F. *J. Catal.* **1990**, *122*, 178.
(9) Peterson, M. W.; Turner, J. A.; Nozik, A. J. *J. Phys. Chem.* **1991**, *95*, 221.
(10) Fox, M. A.; Dulay, M. T. *Chem. Rev.* **1993**, *93*, 341.
(11) Carraway, E. R.; Hoffmann, A. J.; Hoffmann, M. R. *Environ. Sci. Technol.* **1994**, *28*, 786.
(12) Ohno, T.; Sarukawa, K.; Matsumura, M. *J. Phys. Chem. B* **2001**, *105*, 2417.
(13) Fu, X.; Clark, L. A.; Yang, Q.; Anderson, M. A. *Environ. Sci. Technol.* **1996**, *30*, 647.
(14) Hirano, K.; Suzuki, E.; Ishikawa, A.; Moroi, T.; Shiroishi, H.; Kaneko, M. *J. Photochem. Photobiol., A* **2000**, *136*, 157.
(15) (a) Herrmann, J.-M.; Disdier, J.; Pichat, P. *J. Phys. Chem.* **1986**, *90*, 6028. (b) Sclafani, A.; Herrmann, J.-M. *J. Photochem. Photobiol., A* **1998**, *113*, 181.
(16) Bahnemann, D. W.; Mönig, J.; Chapman, R. *J. Phys. Chem.* **1987**, *91*, 3782.
(17) Park, V. N.; Ventov, N. G. *Russ. J. Phys. Chem.* **1975**, *49*, 1489.
(18) Meites, T.; Meites, L. *Anal. Chem.* **1955**, *27*, 1531.
(19) Martin, S. T.; Kesselman, J. M.; Park, D. S.; Lewis, N. S.; Hoffmann, M. R. *Environ. Sci. Technol.* **1996**, *30*, 2535.
(20) Choi, W.; Hoffmann, M. R. *J. Phys. Chem.* **1996**, *100*, 2161.
(21) Robinson, E. A. *J. Chem. Soc.* **1961**, 1663.
(22) Choi, Y.-K.; Seo, S.-S.; Chjo, K.-H.; Choi, Q.-W.; Park, S.-M. *J. Electrochem. Soc.* **1992**, *139*, 1803.
(23) Wardman, P. *J. Phys. Chem. Ref. Data* **1989**, *18*, 1637.
(24) Nishimoto, S.; Ohtani, B.; Kagiya, T. *J. Chem. Soc., Faraday Trans. 1* **1985**, *81*, 2467.
(25) Choi, W.; Hoffmann, M. R. *Environ. Sci. Technol.* **1995**, *29*, 1646.
(26) Bahnemann D. W.; Kholuiskaya, S. N.; Dillert, R.; Kulak, A. I.; Kokorin, A. I. *Appl. Catal. B* **2002**, *36*, 161.
(27) Grätzel, M. *Acc. Chem. Res.* **1981**, *14*, 376.
(28) Yamakata, A.; Ishibashi, T.; Onishi, H. *J. Phys. Chem. B* **2001**, *105*, 7258.